REGULAR PAPERS

Planar structured perovskite solar cells by hybrid physical chemical vapor deposition with optimized perovskite film thickness

Japanese Journal of Applied Physics **57**, 052301 (2018)
https://doi.org/10.7567/JJAP.57.052301

REGULAR PAPER

Planar structured perovskite solar cells by hybrid physical chemical vapor deposition with optimized perovskite film thickness

Xiangyang Wei[1], Yanke Peng[1], Gaoshan Jing[1*], and Tianhong Cui[2*]

[1]*State Key Laboratory of Precision Measurement Technology and Instruments, Department of Precision Instrument, Tsinghua University, Beijing 100084, China*
[2]*Department of Mechanical Engineering, University of Minnesota, Minneapolis, MN 55455, U.S.A.*

*E-mail: gaoshanjing@mail.tsinghua.edu.cn; tcui@me.umn.edu

Received November 25, 2017; accepted February 21, 2018; published online April 10, 2018

The thickness of perovskite absorber layer is a critical parameter to determine a planar structured perovskite solar cell's performance. By modifying the spin coating speed and PbI_2/*N*,*N*-dimethylformamide (DMF) solution concentration, the thickness of perovskite absorber layer was optimized to obtain high-performance solar cells. Using a PbI_2/DMF solution of 1.3 mol/L, maximum power conversion efficiency (*PCE*) of a perovskite solar cell is 15.5% with a perovskite film of 413 nm at 5000 rpm, and *PCE* of 14.3% was also obtained for a solar cell with a perovskite film of 182 nm thick. It is derived that higher concentration of PbI_2/DMF will result in better perovskite solar cells. Additionally, these perovskite solar cells are highly uniform. In 14 sets of solar cells, standard deviations of 11 sets of solar cells were less than 0.50% and the smallest standard deviation was 0.25%, which demonstrates the reliability and effectiveness of hybrid physical chemical vapor deposition (HPCVD) method.

1. Introduction

Solar cells based on hybrid inorganic–organic perovskite material have generated huge interest in recent years in photovoltaic (PV) research field due to perovskite's superior photoelectric conversion properties and low material cost.[1,2] Since a liquid electrolyte based perovskite solar cell was developed at Miyasaka research group with a power conversion efficiency (*PCE*) of 3.8%,[3] *PCE*s of perovskite solar cells have increased drastically in recent years. In 2017, the certificated perovskite *PCE* already reached 22.7%, which is higher than that of a CdTe solar cell, much more than that of an amorphous silicon solar cell (14%) and close to that of a single crystalline silicon solar cell (25.4%).[4] Compared to the theoretical limit of the single crystalline silicon solar cell's *PCE*, 29.8%,[5] the theoretical limit of the perovskite solar cell's *PCE* could reach 31% and there is still plenty of room for improvement.[6] A great challenge for perovskite solar cell research is to develop a simplified structured solar cell with processing parameters precisely controlled to obtain a uniform *PCE* at large scale.[2] Through this way, the fabrication process to make perovskite cells could be further optimized with higher power conversion efficiency and perovskite cells could compete with commercially available solar cells without government subsidy, especially CdTe solar cells.[2]

Typically, a perovskite solar cell is composed of three components: an electron transfer layer, a light absorption layer of perovskite for generating electrons and holes, and a hole transfer layer.[7] The TiO_2 thin film is a commonly utilized electron transfer layer.[7] There are drawbacks for TiO_2 film as the electron transfer layer: electron mobility in a TiO_2 film is low with high electron-trap state density in the conduction band, which will decrease the solar cell's *PCE* and long-term stability.[8–10] Meanwhile, perovskite solar cells based on TiO_2 electron transport layer generally demonstrate a characteristic large hysteresis.[11–14] In order to reduce the perovskite solar cell's hysteresis, an additional layer of thin film was deposited on the electron transfer layer to form a combined electron transfer layer. For instance, a mesoporous TiO_2 layer was coated over a compact TiO_2 electron transfer layer to increase the contact area between the combined TiO_2 electron transfer layer and the light absorption layer, so the transfer rate of photo-generated electron inside the light absorption layer of perovskite could be accelerated.[15–18] Nevertheless, such an auxiliary film will increase the complexity of a perovskite solar cell's structure and fabrication process, and further increase the cost of the perovskite solar cells.

Planar structured perovskite solar cells have also been constructed to thoroughly investigate the photo-conversion mechanism inside perovskite solar cells due to the simplified solar cell structure.[19] A planar structured perovskite solar cell could be classified as a p–i–n solar cell and a commonly investigated planar structured solar cell is composed of three sequentially connected thin films: a compact TiO_2 film as the electron transfer layer, a perovskite film as the light absorption layer and 2,2′,7,7′-tetrakis(*N*,*N*-di-p-methoxyphenylamine)-9,9′-spirobifluorene (spiro-OMeTAD) as the hole transfer layer. So far as we know, the highest *PCE* achieved for such planar structured perovskite solar cell said above is 19.4% by obtaining high-quality perovskite film using solution based "one-step" method.[20] To obtain high-quality perovskite film and increase the solar cell's *PCE*, anhydrous chlorobenzene was added during the spin coating process to accelerate solvent evaporation and increase the grain size of perovskite film. There are several disadvantages of solution-based methods to get high-quality perovskite film uniformly: poor process control and contamination induced during the synthesis process.[21–24] Several vapor-based methods have been introduced to synthesize high-quality perovskite film. In our previous publication, a hybrid physical and chemical vapor deposition method (HPCVD) has been applied to fabricate a highly stable perovskite solar cell with a maximum efficiency of 14.7%, with a combined compact/mesoporous TiO_2 electron transfer layer. After 31 days' testing, the solar cell can still maintain its *PCE* at 12.1%.[25] Dual source evaporation method has been used to fabricate a planar structured solar cell with a *PCE* of 15.4% using two precursors: CH_3NH_3I and $PbCl_2$.[26] In addition, CVD process with a multi-zone tube furnace has been utilized to obtain a planar structured perovskite with a *PCE* of 11.8% using two precursors: CH_3NH_3I and $PbCl_2$.[27] With a high-quality TiO_2

compact electron transfer layer by E-beam evaporation, a planar structured $CH_3NH_3I_{3-x}Cl_x$ perovskite solar cell with a *PCE* of 16.8% was fabricated in a high-pressure CVD furnace at 120 °C.[28] Meanwhile, a low-pressure CVD method was used, combined with a high-quality TiO_2 film by high-temperature spray pyrolysis method, to make a solar cell with a *PCE* of 15.37%.[29] Though vapor based methods have not been widely used in perovskite solar cell research field, high performance planar structured perovskite solar cells based on high-quality perovskite film could be manufactured in large scale with these methods.

Additionally, the thickness of perovskite absorber layer is a crucial parameter to determine the perovskite solar cell's performance, which is affected by the precursor's thickness, e.g., PbI_2. Theoretically, a photo-generated carrier's diffusion length in a perovskite film is larger than one micron.[30] Due to the difficulty to measure the carrier diffusion length in a perovskite film precisely, the thickness of perovskite absorber layer has been investigated to characterize the film quality. It has been demonstrated that an optimum perovskite film thickness exists for different solar cell fabrication designs and methods, which is well below one micron. For a planar structured solar cell based on a methylammonium lead iodide perovskite film using a dual-source thermal evaporation method, the optimum thickness of the perovskite film is about 300 nm in the range of 160 to 900 nm. Eventually, the perovskite film is sandwiched between two organic charge transporting layers and the highest *PCE* obtained for the 300 nm perovskite film is 12.7%.[31] For a planar structured solar cell with a structure of $ZnO/CH_3NH_3PbI_3/P_3HT$, the optimum perovskite film thickness is about 330 nm, at which *PCE* up to 11.3% was obtained for a perovskite solar cell for vapor based method.[32] For a planar structured solar cell based on a $CH_3NH_3PbI_{3-x}Cl_x$ perovskite layer, optimum perovskite film of 575 nm will yield devices with efficiencies of up to 11.88%.[33] Typically, a larger thickness of the light absorption layer will lead to larger light absorption and photo-generation carriers. Meantime, a larger thickness of light absorption layer will lead to deterioration of the solar cell's parameters related to perovskite film quality, such open circuit voltages (V_{oc}) and filling factor (*FF*).[31] Due to the variation of perovskite film fabrication methods, it is still quite challenging to find the universal rule to govern the optimization process for the perovskite film thickness for a certain vapor based method.

In this paper, simplified planar structured perovskite solar cells were fabricated by HPCVD method with a compact TiO_2 film as the electron transfer layer, $CH_3NH_3PbI_3$ as the light absorption layer and spiro-OMeTAD as the hole transfer layer. Two critical parameters, spin coating speed and PbI_2 concentration, were thoroughly investigated to obtain the optimum perovskite film quality and thickness. Maximum *PCE* of a perovskite solar cell was 15.5% and *PCE* of 14.3% was also obtained for a solar cell with a 182-nm-thick perovskite film using a PbI_2 concentration of 0.8 mol/L at 5000 rpm. From our experimental results, a perovskite film's quality and thickness are determined by the PbI_2 concentration, as well as spin coating speed, which will further determine a planar perovskite solar cell's *PCE*. Using a PbI_2 precursor solution with a certain concentration, higher spin coating speed will lead to PbI_2 film with better quality, which results in higher quality perovskite film and higher V_{oc}. Higher PbI_2 concentration will lead to a larger thickness of PbI_2, which results in a larger thickness of perovskite film and larger short circuit current (J_{sc}). Meantime, higher spin coating speed will lead to a smaller thickness of PbI_2, which results in a smaller thickness of perovskite film and smaller J_{sc}. Combined with these two parameters, the champion solar cell with a *PCE* of 15.5% was obtained using a PbI_2 concentration of 1.3 mol/L at 5000 rpm. Highly uniform perovskite solar cells were achieved with a standard deviation less than 0.74%. Such experimental results could be utilized to further optimize various methods to synthesize planar structured perovskite solar cells. It also demonstrates that HPCVD method is a highly reliable technique to make high-performance perovskite solar cells and could result in mass productions of perovskite solar cells in the near future.

2. Experimental methods

2.1 Substrate preparation

First, precision laser etching technique was used to pattern the fluorine-doped tin oxide (FTO) transparent conductive glass substrates (Nippon Sheet Glass, 14 Ω). Then, the FTO glass substrates were cleaned with deionized (DI) water, ethanol, acetone, and isopropyl alcohol (IPA) sequentially for 30 min in an ultrasonic bath. Next, 15 min of oxygen plasma treatment (Henniker Plasma PDC-32G-2) was applied to eliminate organic residues on surfaces of the FTO glass substrates.

2.2 Solar cells fabrication

A compact TiO_2 layer was deposited on the FTO glass by spin coating method at 2000 rpm (Brewer Science, 200X) according to the previous publication.[34] The compact TiO_2 film was baked at 100 °C for 15 min and then was sintered at 500 °C for 30 min in a muffle furnace (Nabertherm, L9/11/P330). After sintering, the compact TiO_2 film was cleaned by a nitrogen gas gun and subsequent a five min of oxygen plasma treatment (Henniker Plasma PDC-32G-2). Firstly, three different concentrations of PbI_2/*N*,*N*-dimethylformamide (DMF; Sigma) solution (0.8, 1.0, and 1.3 mol/L) were prepared by stirring at 100 °C and were purified separately filtered by 22 μm nylon filters (JINTENG, nylon 66 $|\varphi = 13$ mm|). PbI_2 films were then deposited on FTO glass substrates by spin coating the different PbI_2/DMF solution separately at different speeds: 1000, 2000, 3000, 4000, and 5000 rpm. During the spin coating process, nitrogen gas flow was applied to increase evaporate rate of DMF solvent. Then the PbI_2 precursor films were obtained by heating at 70 °C for 20 min. To be noted, uneven PbI_2 film was obtained for a 1.3 mol/L PbI_2/DMF solution at 1000 rpm, so perovskite solar cells based on such PbI_2 film were not available in this paper.

Then, the perovskite film was fabricated by an HPCVD process.[25] Briefly, the substrates with PbI_2 films were loaded into a customized quartz tube evenly distributed with CH_3NH_3I powder (Dyesol Industries). Then, the quartz tube was pumped to a vacuum level of 80 mTorr, and heated to 105 °C for six hours with a pre-configured program. During the process, PbI_2 films were completely transformed to $CH_3NH_3PbI_3$ films at an environment filled with CH_3NH_3I vapor. As shown in Fig. S1 in the online supplementary data at http://stacks.iop.org/JJAP/57/052301/mmedia, the crystalline phase of PbI_2 can be verified in the X-ray diffraction

(XRD) patterns of $PbI_2/TiO_2/FTO$/glass substrate at a series of angles of 12.6, 25.4, 38.6, 39.5, and 52.3°. However, after the synthesis process by HPCVD, all these five degrees disappear in the XRD spectra of $CH_3NH_3PbI_3$ (0.8 mol/L, 5000 rpm, 182 nm)/TiO_2/FTO/Glass substrate and $CH_3NH_3PbI_3$ (1.3 mol/L, 5000 rpm, 413 nm)/TiO_2/FTO/Glass substrate, indicating all the PbI_2 having converted to perovskite film of $CH_3NH_3PbI_3$. After that, the substrates with $CH_3NH_3PbI_3$ films were taken out of the quartz tube and $CH_3NH_3PbI_3$ films were further annealed at 100 °C for 10 min. Next, a spiro-OMeTAD (Lumtech) film was coated on the $CH_3NH_3PbI_3$ film by spin coating at 6000 rpm according to the previous publication.[35] Finally, a 70 nm thick gold layer was deposited by thermal evaporation (SKY Technology Development) on the spiro-OMeTAD film using a stainless steel shadow mask.

2.3 Solar cells characterization

The thicknesses of $CH_3NH_3PbI_3$ films were measured by a profilometer (Veeco Dektak 150) with a resolution ratio of 0.1 nm at a measurement range of 6.5 μm. Surface profiles of the $CH_3NH_3PbI_3$ films and cross-section of the perovskite solar cells were characterized by a field-emission scanning electron microscope (FE-SEM; Zeiss Merlin). A semiconductor device parameter analyzer (Keysight B1500A) was utilized to measure the current density–voltage (*J–V*) curves of perovskite solar cells. The *J–V* curves of the perovskites solar cells were measured under simulated AM 1.5 illumination with a 9 mm^2 stainless steel mask covered on the solar cells. A solar simulator (Newport 94021A) was used to form the illumination situation, which was calibrated by a mono-silicon reference cell (Newport calibration cert, #0702). Voltage scanning configuration of *J–V* curves was set from 1.2 to −0.1 to 1.2 V, with a 50 mV step and 50 ms delay.

3. Results and discussion

A planar structured perovskite solar cell can be classified as a type of p–i–n solar cells,[2] such as polysilicon, CdTe etc., with the electron transfer layer of TiO_2 as a n-type semiconductor layer, the light absorption layer of perovskite as an intrinsic semiconductor layer, and the hole transfer layer of spiro-OMeTAD as a p-type semiconductor layer. Our hypothesis is that such a planar perovskite solar cell should follow the rules for another conventional p–i–n thin film solar cells.[19] There should be an optimized thickness for the light absorption layer of perovskite to get a maximum *PCE*. The perovskite film thickness should be large enough to absorb most incident light and generate electron/hole pairs. Meanwhile, the thickness should be small enough to minimize the electron and hole recombination with the defects inside the perovskite film induced by fabrication processing. Two critical parameters, spin coating speed and PbI_2 concentration, were thoroughly investigated to obtain the optimum perovskite film quality and thickness for a high performance perovskite solar cell.

3.1 Thickness of perovskite film

A PbI_2 precursor film's thickness and film quality determine the $CH_3NH_3PbI_3$ film's thickness and quality. By adjusting the processing parameters affecting PbI_2 precursor film's thickness and film quality, optimizing scheme could be derived from the planar perovskite solar cell based on our highly reliable HPCVD method. The thickness of PbI_2 precursor film can be adjusted by modifying two critical parameters: spin coating speed and PbI_2/DMF solution concentration. PbI_2/DMF solutions with different concentration were made for the optimization process, 0.8, 1.0, and 1.3 mol/L. A series of high quality, homogeneous PbI_2 precursor films were obtained by modifying spin coating speed from 1000 to 5000 rpm for these solutions based on our previous publication.[36] Then, corresponding perovskite solar cells were fabricated using highly reliable HPCVD method.[25] As expected higher PbI_2/DMF concentration and lower spin coating speed result in a thicker PbI_2 film shown in Fig. 1, which results in thicker perovskite film. We obtained $CH_3NH_3PbI_3$ thin films with 603, 493, 450, and 413 nm at 2000, 3000, 4000, and 5000 rpm, respectively, for a 1.3 mol/L PbI_2/DMF solution. While for a 1.0 mol/L PbI_2/DMF solution, 370, 304, 272, and 250 nm thick perovskite films were obtained at 2000, 3000, 4000, and 5000 rpm, respectively. When the concentration of PbI_2/DMF decreased to 0.8 mol/L, 297, 255, 215, and 182 nm thick perovskite films were obtained at 2000, 3000, 4000, and 5000 rpm, respectively.

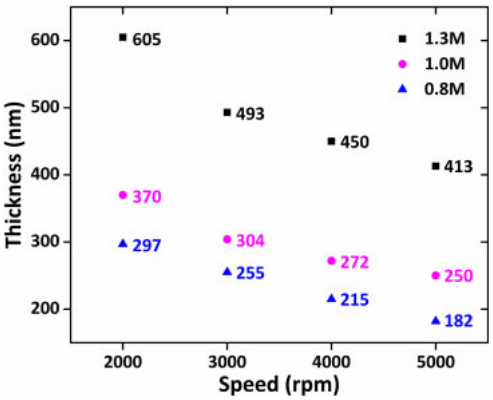

Fig. 1. (Color online) Thickness of $CH_3NH_3PbI_3$ films obtained by HPCVD method based on PbI_2/DMF solutions with different concentrations (0.8, 1.0, and 1.3 mol/L) spin coated at 2000, 3000, 4000, and 5000 rpm, respectively.

3.2 Quality of perovskite film

Quality of perovskite film fabricated by HPCVD method can be characterized by two parameters: number of perovskite crystal grains in the vertical direction and number of pinholes in the planar direction of a perovskite solar cell. The number of crystal grains in the vertical direction is correlated with the perovskite film thickness. The lower number of perovskite crystal grains in the vertical direction, the better the film quality. A typical grain size of the perovskite films fabricated by HPCVD process is in a range of 200 to 300 nm. For a perovskite film with a thickness of 180 nm shown in Fig. 2(a), there distributed far more single perovskite crystal gains in the vertical direction. While for a perovskite film with a thickness of 493 nm shown in Fig. 2(b), there distributed quite a few polycrystalline grains in the vertical direction. Correspondingly, the vertical direction is where carries transport from the electron transfer layer to the hole transfer layer. According to classical semiconductor theory, grain boundaries between these polycrystalline will greatly impede carriers transporting and deteriorate the solar cell's performance.[37] Therefore, perovskite film with smaller thickness is superior to the film with larger thickness from the quality point.

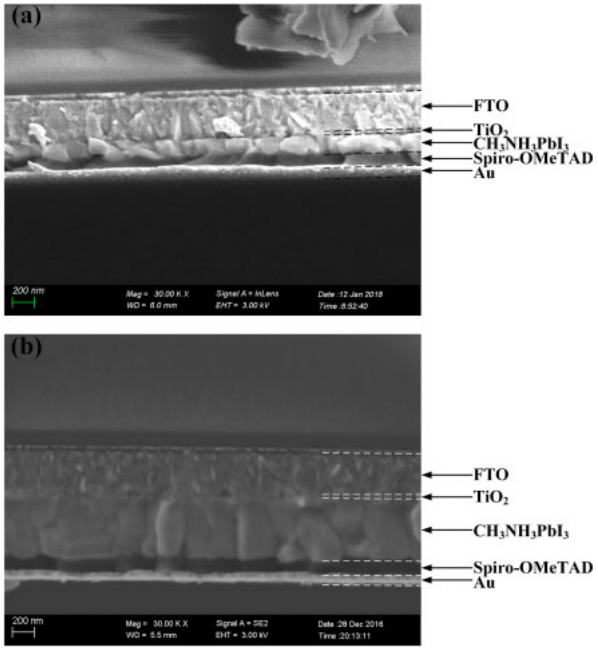

Fig. 2. (Color online) Cross-sectional view SEM image of a planar structured perovskite solar cell by HPCVD based on (a) a 0.8 mol/L PbI_2/DMF solution spin coated at 5000 rpm with a 182-nm-thick $CH_3NH_3PbI_3$ film and (b) a 1.3 mol/L PbI_2/DMF solution spin coated at 3000 rpm with a 493-nm-thick $CH_3NH_3PbI_3$ film.

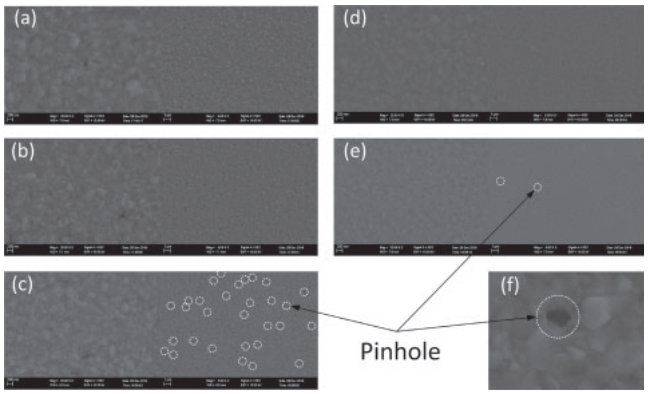

Fig. 3. Top view SEM images of $CH_3NH_3PbI_3$ films based on PbI_2 films spin coated at (a) 1000, (b) 2000, (c) 3000, (d) 4000, and (e) 5000 rpm for a 1.0 mol/L PbI_2/DMF solution; (f) magnified top view SEM image of a single pinhole. (a)–(e) Left part of the images are taken with higher magnification than the right part.

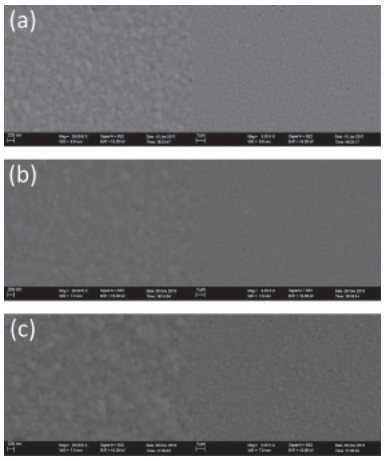

Fig. 4. Top view SEM images of $CH_3NH_3PbI_3$ films based on PbI_2 films spin-coated with an (a) 0.8, (b) 1.0, and (c) 1.3 mol/L PbI_2/DMF solution at 4000 rpm. The left part of the images is taken with higher magnification than the right part.

Meanwhile, film quality can also be characterized by the number of pinholes in the planar direction of a perovskite solar cell. The number of pinholes in the planar direction is correlated with PbI_2 precursor spin coating speed and PbI_2 concentration. Higher spin coating speed will improve the PbI_2 film's uniformity and quality, which will result in better quality of perovskite film. As shown in Fig. 3, average perovskite film's grain sizes decrease due to the increase in spin coating speed. At higher spin-coating speed, uniformly smaller grain sizes of perovskite films were obtained, as well as fewer pinholes. At 5000 rpm, almost no pinholes were observed on the perovskite film surface at 20,000 amplification shown in Fig. 3. One feasible explanation is that DMF solvent evaporation rate is larger at higher spin-coating speed, which accelerates the film forming of the PbI_2 precursor film. Due to the higher solvent evaporation rate, smaller grain sized PbI_2 precursor film forms. As for the mechanism of the smaller grain sizes obtained from high spin-coating speed, it could be explained by the following principle: at higher spin-coating speed, the nucleation rate is faster than that of slower spin-coating speed. This means more nuclei will be generated, which will lead to smaller grain size after the crystallization process. Meanwhile, higher DMF solution evaporation rate leads to fewer pinholes and more uniform PbI_2 precursor film from our previous publication.[34] Eventually, smaller, but more uniform grain sized perovskite films were obtained at higher spin coating speed.

Higher PbI_2/DMF concentration will also improve the PbI_2 film's uniformity and quality. Here, we chose three PbI_2/DMF concentration, 1.3, 1.0, and 0.8 mol/L at 4000 rpm to investigate its effect on solar cells' performance. As shown in Fig. 4, average perovskite film's grain sizes gradually increase with the increase of PbI_2 solution concentration, as well as with fewer pinholes on the film surface. For perovskite film from a 1.3 mol/L PbI_2 solution, almost no pinholes were observed on the perovskite film surface at 20,000 amplification, while there were still a few pinholes on the perovskite film from 1.0 and 0.8 mol/L PbI_2/DMF solutions. Higher PbI_2/DMF concentration resulted in more dense PbI_2 film with much less pinholes and better quality perovskite film of 450 nm thick was obtained with 1.3 mol/L PbI_2/DMF solution.

3.3 Relation between the thickness, quality of perovskite film and solar cell performance

A perovskite solar cell by HPCVD method is highly determined by the thickness and quality of perovskite absorber layer. For instance, as for a $CH_3NH_3PbI_3$ film of 493 nm with PbI_2 film spin coated at 3000 rpm for a 1.3 mol/L PbI_2/DMF solution, this solar cell's *PCE* is 14.6% with reverse scan: $J_{sc} = 21.29\,mA/cm^2$, $V_{oc} = 1.02\,V$, and $FF = 0.67$. On the contrast for a $CH_3NH_3PbI_3$ film of 182 nm with PbI_2 film spin coated at 5000 rpm for a 0.8 mol/L PbI_2/DMF solution, this solar cell's *PCE* is 14.3% with reverse scan: $J_{sc} = 18.24\,mA/cm^2$, $V_{oc} = 1.02\,V$, and $FF = 0.75$. Even these two solar cells' *PCE*s are close, the solar cell with thin perovskite film (182 nm) achieves larger *FF* (0.75 vs 0.67) with less short

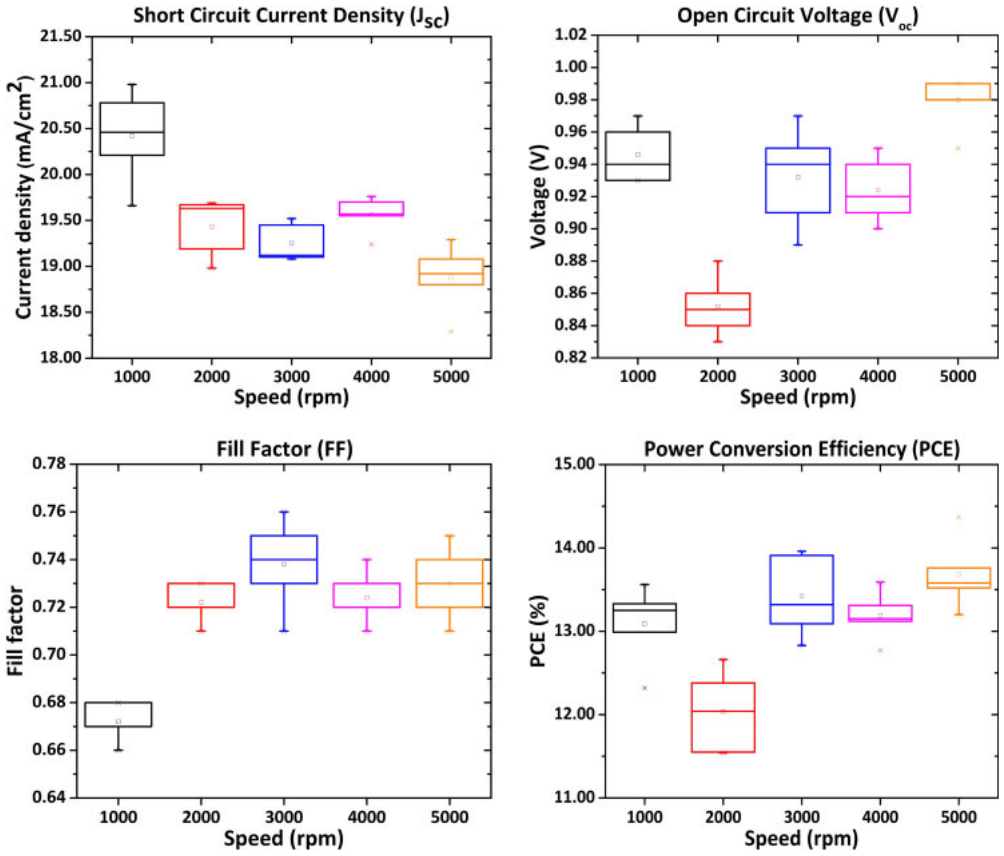

Fig. 5. (Color online) J_{sc}, V_{oc}, *FF*, and *PCE* statistics of perovskite solar cells with $CH_3NH_3PbI_3$ films based on PbI_2 films spin coated at 1000, 2000, 3000, 4000, and 5000 rpm for a 1.0 mol/L PbI_2/DMF solution.

circuit current (18.24 mA/cm^2 vs 21.29 mA/cm^2). A plausible explanation is that the planar perovskite solar cell can be treated as a conventional p–i–n thin film solar cell. The p–i–n solar cell's short circuit current, J_{sc}, is highly determined by the thickness of light absorption layer with similar film quality.[19] Indeed, it is demonstrated by our experimental results shown in Figs. 5 and 6. Higher spin coating speed leads to smaller J_{sc} due to the decreased light absorption layer of perovskite film. Average J_{sc} at 5000 rpm is 18.88 mA/cm^2, which is much smaller than average J_{sc} at 1000 rpm, 20.42 mA/cm^2. In contrast, higher spin coating speed leads to larger V_{oc} and *FF* due to the improved film quality of perovskite film. At 1000 rpm, the average V_{oc} and *FF* are 0.95 V and 0.67, respectively. Correspondingly, the average V_{oc} and *FF* are 0.98 V and 0.73 at 5000 rpm. Eventually, a solar cell's efficiency (*PCE*) is balanced by the perovskite film thickness and quality. The highest average efficiency of 13.7% is obtained at 5000 rpm, while the smallest average efficiency of 12.0% is obtained at 2000 rpm.

The larger PbI_2/DMF solution at higher spin coating speed will further improve the perovskite solar cell's performance. As shown in Table I, the largest J_{sc} for a 0.8 mol/L PbI_2/DMF solution was 19.89 mA/cm^2 at 1000 rpm, while the largest V_{oc} and *FF* were 1.02 V and 0.75 at 5000 rpm. The largest *PCE* obtained for a 0.8 mol/L PbI_2/DMF solution was 14.3% at 5000 rpm. Similar results were shown in Table II, the largest J_{sc} for 1.0 mol/L PbI_2/DMF solution was 20.98 mA/cm^2 at 1000 rpm, while the largest V_{oc} and the second largest *FF* were 0.99 V and 0.75 at 5000 rpm. The largest *PCE* obtained for 1.0 mol/L PbI_2/DMF solution was

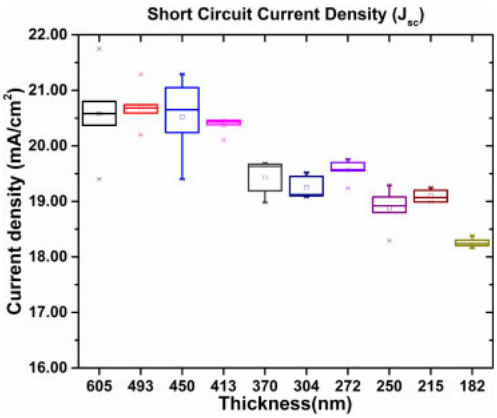

Fig. 6. (Color online) J_{sc} statistics of perovskite solar cells throughout the whole $CH_3NH_3PbI_3$ films' thickness with a series of 605, 493, 450, 413, 370, 304, 272, 250, 215, and 182 nm.

14.4% at 5000 rpm. For 1.3 mol/L PbI_2/DMF solution shown in Table III, the largest J_{sc} was 21.75 mA/cm^2 at 1000 rpm, while the largest V_{oc} and *FF* were 1.04 V and 0.73 at 5000 rpm. The highest *PCE* obtained for a 1.3 mol/L PbI_2/DMF solution was 15.5% at 5000 rpm. Even with the fluctuation of solar cells' *PCE*s, we deduced that highest *PCE* can be obtained with a higher concentration of the PbI_2/DMF solution (1.3 M) at a higher spin coating speed (5000 rpm). Ideally, even higher *PCE* could be achieved for higher PbI_2/DMF concentration greater than 1.3 mol/L at 5000 rpm. Though in our experiment, 1.3 mol/L PbI_2/DMF concentration was the highest we could obtain and the higher PbI_2/

Table I. Statistics of perovskite solar cells by HPCVD with 0.8 mol/L PbI_2/DMF solution at different spin coating speed. Note: largest *PCE*, J_{sc}, V_{oc}, and *FF* are highlighted in bold.

Speed (rpm)	*PCE* (%)	J_{sc} (mA/cm^2)	V_{oc} (V)	*FF*
1000	14.0	19.70	0.98	0.71
1000	13.8	19.63	0.97	0.71
1000	13.3	19.60	0.96	0.69
1000	13.2	**19.89**	0.94	0.69
1000	12.7	19.58	0.91	0.69
2000	13.3	19.24	0.95	0.71
2000	12.6	18.94	0.93	0.70
2000	12.6	19.34	0.89	0.71
2000	12.0	19.40	0.86	0.70
2000	11.8	19.15	0.87	0.69
3000	13.4	18.54	0.95	0.74
3000	12.8	18.96	0.90	0.73
3000	12.6	18.70	0.92	0.72
3000	12.4	19.07	0.91	0.70
3000	11.1	18.69	0.84	0.69
4000	13.2	19.20	0.95	0.71
4000	13.1	18.99	0.94	0.71
4000	12.9	19.25	0.91	0.72
4000	12.8	18.99	0.93	0.71
4000	11.8	19.07	0.87	0.69
5000	**14.3**	18.24	**1.02**	**0.75**
5000	13.5	18.20	1.01	0.72
5000	13.4	18.30	0.99	0.72
5000	13.0	18.16	0.99	0.71
5000	12.9	18.38	0.96	0.72

Table II. Statistics of perovskite solar cells by HPCVD with 1.0 mol/L PbI_2/DMF solution at different spin coating speed. Note: largest *PCE*, J_{sc}, V_{oc}, and *FF* are highlighted in bold.

Speed (rpm)	*PCE* (%)	J_{sc} (mA/cm^2)	V_{oc} (V)	*FF*
1000	13.6	20.46	0.96	0.68
1000	13.3	20.21	0.97	0.68
1000	13.3	20.78	0.94	0.67
1000	13.0	**20.98**	0.93	0.66
1000	12.3	19.66	0.93	0.67
2000	12.7	19.63	0.88	0.73
2000	12.4	19.69	0.86	0.72
2000	12.0	19.67	0.85	0.72
2000	11.6	18.98	0.83	0.73
2000	11.5	19.19	0.84	0.71
3000	14.0	19.08	0.97	0.75
3000	13.9	19.12	0.94	**0.76**
3000	13.3	19.52	0.91	0.74
3000	13.1	19.10	0.95	0.71
3000	12.8	19.45	0.89	0.73
4000	13.6	19.57	0.95	0.73
4000	13.3	19.76	0.94	0.71
4000	13.2	19.70	0.92	0.72
4000	13.1	19.24	0.91	0.74
4000	12.8	19.55	0.90	0.72
5000	**14.4**	19.29	**0.99**	0.74
5000	13.8	18.92	**0.99**	0.72
5000	13.6	18.80	0.98	0.73
5000	13.5	19.08	**0.99**	0.71
5000	13.2	18.29	0.95	0.75

Table III. Statistics of perovskite solar cells by HPCVD with 1.3 mol/L PbI_2/DMF solution at different spin coating speed. Note: largest *PCE*, J_{sc}, V_{oc}, and *FF* are highlighted in bold.

Speed (rpm)	*PCE* (%)	J_{sc} (mA/cm^2)	V_{oc} (V)	*FF*
2000	14.0	**21.75**	1.01	0.63
2000	13.9	20.80	0.99	0.67
2000	13.7	20.37	1.01	0.66
2000	13.5	20.58	0.95	0.69
2000	13.3	19.40	0.99	0.68
3000	14.6	21.29	1.02	0.67
3000	14.3	20.59	1.02	0.68
3000	13.9	20.74	1.02	0.65
3000	13.5	20.68	1.00	0.65
3000	13.2	20.20	0.94	0.69
4000	15.2	21.29	1.01	0.70
4000	14.5	20.65	1.00	0.70
4000	14.5	21.05	1.02	0.67
4000	14.4	20.24	1.00	0.71
4000	14.0	19.40	1.00	0.71
5000	**15.5**	20.46	1.03	**0.73**
5000	15.1	20.43	1.02	0.72
5000	14.7	20.38	**1.04**	0.70
5000	14.6	20.46	**1.04**	0.69
5000	14.1	20.11	1.03	0.67

DMF solution would result in unsolvable PbI_2 inside the DMF solvent, which would be greatly detrimental to spin coating process.

Specifically, perovskite solar cells with better performance were obtained with a 1.3 mol/L PbI_2/DMF solution. As shown in Fig. 7, we obtained $CH_3NH_3PbI_3$ thin films with 450, 272, and 215 nm at 4000 rpm for 1.3, 1.0, and 0.8 mol/L PbI_2/DMF solutions, respectively. These perovskite solar cells also demonstrated the characteristic properties of a typical p–i–n thin film solar cell. Larger thickness led to higher J_{sc} due to the increased light absorption of perovskite film. Average J_{sc} for 1.3 mol/L was 20.53 mA/cm^2, while average J_{sc} for 1.0 and 0.8 mol/L were 19.56 and 19.1 mA/cm^2, respectively. Meanwhile, higher V_{oc} was obtained at higher PbI_2 solution due to the improved film quality of the PbI_2 film. Average V_{oc} and *FF* were 1.01 V and 0.70 for 1.3 mol/L, while average V_{oc} and *FF* were 0.92 V/0.72 and 0.92 V/0.71 for 1.0 mol/L, 0.8 mol/L, respectively. Eventually, the highest average efficiency of 14.6% was obtained for 1.3 mol/L at 4000 rpm, while the smallest average efficiency of 12.8% was obtained for 0.8 mol/L at 4000 rpm.

Collectively, an HPCVD based perovskite solar cell's performance and efficiency were determined by the perovskite film's thickness and film quality, which were paradoxical and determined by PbI_2/DMF solution spin coating speed and concentration. Indeed, the planar perovskite solar cell fabricated by HPCVD method demonstrates it is one type of p–i–n solar cells. Similar to polysilicon and CdTe solar cells, such a perovskite solar cell's performance is highly determined by the thickness and quality of the optical absorption film (perovskite film). Meantime, the HPCVD method is vapor based thin film fabrication method for perovskite film, similar to vapor transport deposition (VTD) method for CdTe film.[38] Further improvement and optimization of HPCVD

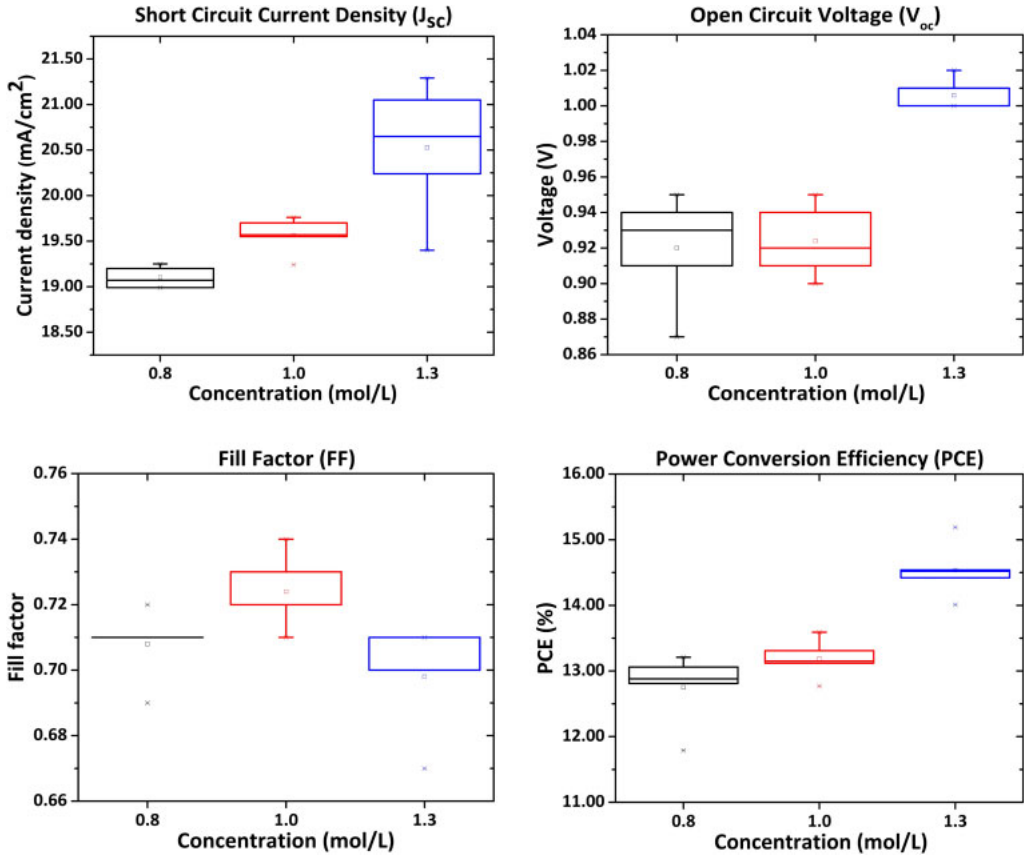

Fig. 7. (Color online) J_{sc}, V_{oc}, *FF*, and *PCE* statistics of perovskite solar cells with $CH_3NH_3PbI_3$ films based on PbI_2 films spin-coated with a 0.8, 1.0, and 1.3 mol/L PbI_2/DMF solution at 4000 rpm.

Table IV. Statistics of perovskite solar cells by HPCVD with PbI_2/DMF solutions (1.3, 1.0, and 0.8 mol/L) at different spin coating speed. Note: lowest standard deviation is highlighted in bold.

Concentration (M)	Speed (rpm)	*PCE* (%)			Standard deviation (%)
		Mean	Max	Min	
1.3	2000	13.6	14.0	13.3	**0.25**
1.3	3000	13.9	14.6	13.2	0.52
1.3	4000	14.6	15.2	14.0	0.38
1.3	5000	14.8	15.5	14.1	0.46
1.0	1000	13.1	13.6	12.3	0.43
1.0	2000	12.0	12.7	11.5	0.44
1.0	3000	13.4	14.0	12.8	0.45
1.0	4000	13.2	14.0	12.8	0.27
1.0	5000	13.7	14.4	13.2	0.39
0.8	1000	13.4	14.0	12.7	0.46
0.8	2000	12.5	13.3	11.8	0.55
0.8	3000	12.4	13.4	11.1	0.74
0.8	4000	12.8	13.2	11.8	0.50
0.8	5000	13.4	14.3	12.9	0.50

method will increase the perovskite film's thickness as well as the film quality.

3.4 Uniformity and hysteresis of our planar structured perovskite solar cells by HPCVD method

Additionally, these planar structured perovskite solar cells by HPCVD were highly uniform. In total, there were 14 sets of perovskite solar cells with each set of solar cells processed under identical conditions. As shown in Table IV, for perovskite solar cells' *PCE*, the standard deviations of the 14 sets of samples were less than 0.74%, of which standard deviations of 11 sets of samples were less than 0.50% and the smallest standard deviation was 0.25%. High uniformity of these perovskite solar cells demonstrated the effectiveness of the HPCVD method and made it feasible for further improvement of the solar cell's performance.

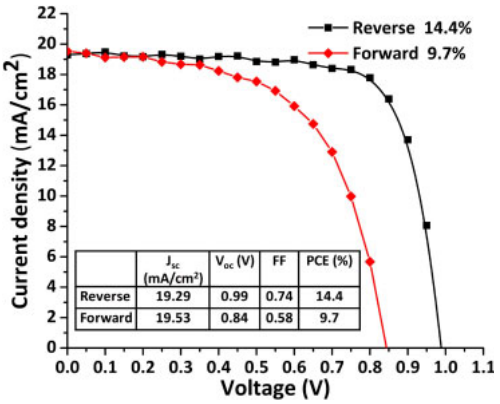

Fig. 8. (Color online) *J*–*V* curve of a $CH_3NH_3PbI_3$ solar cell by HPCVD with hysteresis measured under simulated AM 1.5 sunlight of 100 mW/cm^2 irradiance.

To be noted, hysteresis is still a common issue for perovskite solar cells with TiO_2 as the electron transfer layer,[10] which is also the case for our planar structured perovskite solar cell by HPCVD. For instance, for a perovskite solar cell obtained by PbI_2/DMF solution of 1.0 mol/L at 5000 rpm shown in Fig. 8, with reverse scan: $J_{sc} = 19.29$ mA/cm^2, $V_{oc} = 0.99$ V, $FF = 0.74$, $PCE = 14.4\%$; and with forward

scan: $J_{sc} = 19.53\,mA/cm^2$, $V_{oc} = 0.84\,V$, $FF = 0.58$, $PCE = 9.7\%$.

It has been found that planar perovskite solar cells on a compact TiO_2 electron transfer layer demonstrate far more severe hysteresis than solar cells based on a mesoporous TiO_2 scaffold.[39] It has been deduced that both the compact TiO_2 electron transfer layer and spiro-MeOTAD layer in a planar perovskite solar cell play critical roles in the electrode polarization and result in *J–V* hysteresis.[39] We believe this matter could be greatly reduced by replacing TiO_2 and spiro-MeOTAD with other high-performance carrier transfer layers and better performance could be achieved for planar structured perovskite solar cells by HPCVD.

4. Conclusions

A batch of highly uniform planar structured perovskite solar cells has been fabricated using vapor-based HPCVD method. By modifying the spin coating speed and PbI_2/DMF solution concentration, the thickness of perovskite absorber layer was optimized to obtain high-performance solar cells with the highest *PCE* of 15.5%. During the optimization process, the relation between the perovskite film quality, solar cells' parameters, and spin coating speed, as well as PbI_2/DMF solution concentration, were thoroughly investigated. It is derived that higher concentration of PbI_2/DMF at higher spin coating speed will result in better perovskite solar cells, e.g., PbI_2/DMF of 1.3 mol/L at 5000 rpm. From our experimental result, these planar structured perovskite solar cells demonstrate the typical characteristic of conventional p–i–n solar cells. Additionally, highly uniform perovskite solar cells were obtained using HPCVD method. In 14 sets of solar cells fabricated, the standard deviation of 11 sets of solar cells were less than 0.50% and the smallest standard deviation was 0.25%, which demonstrates the reliability and effectiveness of HPCVD method. In future, such simplified structure perovskite solar cells could be further optimized using HPCVD and could lead to large-scale manufacturing of perovskite solar cells at low cost.

Acknowledgments

This work was financially supported by State Key Laboratory of Precision Measurement Technology and Instruments, Tsinghua University and the International Science and Technology Cooperation Program of Ministry of Science and Technology of the People's Republic of China (Grant No. 2013DFA51800).

1) A. Polman, M. Knight, E. C. Garnett, B. Ehrler, and W. C. Sinke, Science **352**, aad4424 (2016).
2) M. A. Green, A. Ho-Baillie, and H. J. Snaith, Nat. Photonics **8**, 506 (2014).
3) A. Kojima, K. Teshima, Y. Shirai, and T. Miyasaka, J. Am. Chem. Soc. **131**, 6050 (2009).
4) Web [https://www.nrel.gov/pv/assets/images/efficiency-chart.png].
5) T. Tiedje, E. Yablonovitch, G. D. Cody, and B. G. Brooks, IEEE Trans. Electron Devices **31**, 711 (1984).
6) W. E. I. Sha, X. Ren, L. Chen, and W. C. H. Choy, Appl. Phys. Lett. **106**, 221104 (2015).
7) J.-P. Correa-Baena, A. Abate, M. Saliba, W. Tress, T. Jesper Jacobsson, M. Grätzel, and A. Hagfeldt, Energy Environ. Sci. **10**, 710 (2017).
8) E. Hendry, M. Koeberg, B. O'regan, and M. Bonn, Nano Lett. **6**, 755 (2006).
9) G. Yang, H. Tao, P. Qin, W. Ke, and G. Fang, J. Mater. Chem. A **4**, 3970 (2016).
10) K. Wojciechowski, S. D. Stranks, A. Abate, G. Sadoughi, A. Sadhanala, N. Kopidakis, G. Rumbles, C.-Z. Li, R. H. Friend, and A. K.-Y. Jen, ACS Nano **8**, 12701 (2014).
11) H. S. Kim, I. H. Jang, N. Ahn, M. Choi, A. Guerrero, J. Bisquert, and N. G. Park, J. Phys. Chem. Lett. **6**, 4633 (2015).
12) N. K. Noel, A. Abate, S. D. Stranks, E. S. Parrott, V. M. Burlakov, A. Goriely, and H. J. Snaith, ACS Nano **8**, 9815 (2014).
13) H. J. Snaith, A. Abate, J. M. Ball, G. E. Eperon, T. Leijtens, N. K. Noel, S. D. Stranks, J. T.-W. Wang, K. Wojciechowski, and W. Zhang, J. Phys. Chem. Lett. **5**, 1511 (2014).
14) H. Zhou, Q. Chen, G. Li, S. Luo, T. B. Song, H. S. Duan, Z. Hong, J. You, Y. Liu, and Y. Yang, Science **345**, 542 (2014).
15) M. M. Lee, J. Teuscher, T. Miyasaka, T. N. Murakami, and H. J. Snaith, Science **338**, 643 (2012).
16) H.-S. Kim, C.-R. Lee, J.-H. Im, K.-B. Lee, T. Moehl, A. Marchioro, S.-J. Moon, R. Humphry-Baker, J.-H. Yum, and J. E. Moser, Sci. Rep. **2**, 591 (2012).
17) V. Gonzalez-Pedro, E. J. Juarez-Perez, W. S. Arsyad, E. M. Barea, F. Fabregat-Santiago, I. Mora-Sero, and J. Bisquert, Nano Lett. **14**, 888 (2014).
18) S. M. Jain, B. Philippe, E. M. Johansson, B. Park, H. Rensmo, T. Edvinsson, and G. Boschloo, J. Mater. Chem. A **4**, 2630 (2016).
19) J. Nelson, *The Physics of Solar Cells* (Imperial College Press, London, 2003) Chap. 8.
20) H. D. Kim, H. Ohkita, H. Benten, and S. Ito, Adv. Mater. **28**, 917 (2016).
21) B. Conings, L. Baeten, C. De Dobbelaere, J. D'Haen, J. Manca, and H. G. Boyen, Adv. Mater. **26**, 2041 (2014).
22) G. E. Eperon, V. M. Burlakov, P. Docampo, A. Goriely, and H. J. Snaith, Adv. Funct. Mater. **24**, 151 (2014).
23) P.-W. Liang, C.-Y. Liao, C.-C. Chueh, F. Zuo, S. T. Williams, X.-K. Xin, J. Lin, and A. K. Y. Jen, Adv. Mater. **26**, 3748 (2014).
24) D. B. Mitzi, M. Prikas, and K. Chondroudis, Chem. Mater. **11**, 542 (1999).
25) Y. Peng, G. Jing, and T. Cui, J. Mater. Chem. A **3**, 12436 (2015).
26) M. Liu, M. B. Johnston, and H. J. Snaith, Nature **501**, 395 (2013).
27) M. R. Leyden, L. K. Ono, S. R. Raga, Y. Kato, S. Wang, and Y. Qi, J. Mater. Chem. A **2**, 18742 (2014).
28) Y. Li, J. K. Cooper, R. Buonsanti, C. Giannini, Y. Liu, F. M. Toma, and I. D. Sharp, J. Phys. Chem. Lett. **6**, 493 (2015).
29) P.-S. Shen, J.-S. Chen, Y.-H. Chiang, M.-H. Li, T.-F. Guo, and P. Chen, Adv. Mater. Interfaces **3**, 1500849 (2016).
30) S. D. Stranks, G. E. Eperon, G. Grancini, C. Menelaou, M. J. Alcocer, T. Leijtens, L. M. Herz, A. Petrozza, and H. J. Snaith, Science **342**, 341 (2013).
31) C. Momblona, O. Malinkiewicz, C. Roldán-Carmona, A. Soriano, L. Gil-Escrig, E. Bandiello, M. Scheepers, E. Edri, and H. Bolink, APL Mater. **2**, 081504 (2014).
32) D. Liu, M. K. Gangishetty, and T. L. Kelly, J. Mater. Chem. A **2**, 19873 (2014).
33) K. Wang, C. Liu, P. Du, L. Chen, J. Zhu, A. Karim, and X. Gong, Org. Electron. **21**, 19 (2015).
34) J. M. Ball, M. M. Lee, A. Hey, and H. J. Snaith, Energy Environ. Sci. **6**, 1739 (2013).
35) J.-H. Im, I.-H. Jang, N. Pellet, M. Grätzel, and N.-G. Park, Nat. Nanotechnol. **9**, 927 (2014).
36) Y. Peng, G. Jing, and T. Cui, RSC Adv. **5**, 95847 (2015).
37) D. Abou-Ras, T. Kirchartz, and U. Rau, *Advanced Characterization Techniques for Thin Film Solar Cells* (Wiley, New York, 2011) Chap. 11.
38) L. Kranz, S. Buecheler, and A. N. Tiwari, Sol. Energy Mater. Sol. Cells **119**, 278 (2013).
39) B. Chen, M. Yang, S. Priya, and K. Zhu, J. Phys. Chem. Lett. **7**, 905 (2016).

